Am. J. Hum. Genet. 62:890–903, 1998

Refined Genetic Mapping of the Darier Locus to a <1-cM Region of Chromosome 12q24.1, and Construction of a Complete, High-Resolution P1 Artificial Chromosome/Bacterial Artificial Chromosome Contig of the Critical Region

Sarah Monk,[1,*] Anavaj Sakuntabhai,[1,*] Simon A. Carter,[3] Steven D. Bryce,[3] Roger Cox,[1] Louise Harrington,[1] Elaine Levy,[1] Victor L. Ruiz-Perez,[3] Eleni Katsantoni,[3] Ahmer Kodvawala,[3] Colin S. Munro,[5] Susan Burge,[2] Marc Larrègue,[6] Gyula Nagy,[7] Jonathan L. Rees,[4] Mark Lathrop,[1] Anthony P. Monaco,[1] Tom Strachan,[3] and Alain Hovnanian[1]

[1]The Wellcome Trust Centre for Human Genetics, University of Oxford, and [2]Department of Dermatology, Churchill Hospital, Oxford; Departments of [3]Human Genetics and [4]Dermatology, University of Newcastle upon Tyne, Newcastle upon Tyne; [5]Department of Dermatology, Southern General Hospital, Glasgow; [6]Department of Dermatology, La Miletrie Hospital, Poitiers; and [7]"Kaposi Mor" Megyei Korhaz, Borgyogyaszati Osztaly, Kaposvar, Hungary

Summary

Darier disease (DD) (MIM 124200) is an autosomal dominant skin disorder characterized by loss of adhesion between epidermal cells and by abnormal keratinization. We present linkage analysis showing, in four families, key recombination events that refine the location of the DD locus on chromosome 12q23-24.1 to a region of <1 cM. We have constructed a YAC/P1 artificial chromosome (PAC)/bacterial artificial chromosome (BAC)–based physical map that encompasses this refined DD region. The map consists of 35 YAC, 69 PAC, 16 BAC, and 2 cosmid clones that were ordered by mapping 54 anonymous sequence-tagged sites. The critical region is estimated to be 2.4 Mb in size, with an average marker resolution of 37.5 kb. The refinement of the critical interval excludes the *ALDH2, RPL6, PTPN11,* and *OAS* genes, as well as seven expressed sequence tags (ESTs) previously mapped in the DD region. The three known genes (*ATP2A2, PPP1CC,* and *SCA2*) and the 10 ESTs mapped within the critical region are not obvious candidates for the DD gene. Therefore, this detailed integrated physical, genetic, and partial transcript map provides an important resource for the isolation of the DD gene and, possibly, other disease genes.

Received November 5, 1997; accepted for publication January 22, 1998; electronically published April 7, 1998.

Address for correspondence and reprints: Prof. Tom Strachan, Department of Human Genetics, University of Newcastle upon Tyne, Ridley Building, Claremont Place, Newcastle upon Tyne, NE1 7RU, United Kingdom. E-mail: tom.strachan@newcastle.ac.uk or Dr. Alain Hovnanian, The Wellcome Trust Centre for Human Genetics, Windmill Road, Headington, Oxford, OX3 7BN, United Kingdom. E-mail: alain.hovnanian@well.ox.ac.uk

* These authors contributed equally to this work.

0002-9297/98/6203-0022$02.00

Introduction

Darier disease (DD; MIM 124200) is an autosomal dominant skin disorder characterized by loss of adhesion between epidermal cells that is associated with both breakdown of the desmosomal-keratin filament complex and premature keratinization (Burge and Wilkinson 1992). Affected individuals display brown warty papules concentrated in the central trunk, the scalp, the forehead, and the flexures. Nail abnormalities and pits in the palms and soles are common. The disease prevalence has been estimated at 1/55,000, with complete penetrance in adults and variable expressivity (Munro 1992). DD has been reported to be associated with mild mental retardation and with an increase in prevalence of epilepsy and neuropsychiatric disorders (Craddock et al. 1994).

The pathophysiology of the disease is unknown, but histological observations reveal acantholysis (cell separation) in the suprabasal layer of the epidermis, with premature differentiation and hyperkeratinization of the epidermis (Burge and Garrod 1991). Electron-microscope studies reveal a breakdown of the desmosomal-keratin filament complex and suggest that a desmosomal component or an intermediate filament (associated) protein may be involved in the pathophysiology of the disease. However, linkage of DD with known desmosomal components and with the type I and type II keratin gene clusters on chromosomes 17q12-21 and 12q11-13, respectively, has been excluded (Bashir et al. 1993; Goldsmith et al. 1993).

The DD locus has been mapped by linkage analysis to chromosome 12q23-24.1, initially within a 12-cM interval between D12S78 and D12S79 (Bashir et al. 1993; Craddock et al. 1993; Parfitt et al. 1994). Further genetic mapping studies have not revealed any evidence of genetic heterogeneity and have refined the region to

4–5 cM between D12S105 and D12S129 and, subsequently, to a 2-cM interval flanked by D12S234 and D12S129 (Carter et al. 1994; Ikeda et al. 1994; Wakem et al. 1996). This region of chromosome 12q24.1 does not contain any known candidate gene.

In an attempt to more precisely localize the DD gene, we genotyped 41 families, using 23 polymorphic DNA markers between D12S105 and D12S129, including nine new polymorphic repeats. The identification of new recombination events enabled us to refine the DD region to an interval of <1 cM between D12S1339 and D12S2263. We subsequently developed a physical map of the minimal region containing the DD gene, by constructing a high-resolution YAC/PAC/BAC (YAC/P1 artificial chromosome/bacterial artificial chromosome) contig encompassing this region. This contig, which is estimated to be 2.4 Mb in size, contains three identified genes and 10 known expressed sequence tags (ESTs), none of which appears to be a plausible candidate gene for DD.

Subjects, Material, and Methods

Recombination Analysis

Families.—A total of 397 individuals, including 216 affected members from 39 British families, 1 large French family, and 1 large Hungarian family, were included in this study. Eight of these families, including family 4 (referred to as "B" by Carter et al. [1994]) have been published elsewhere (Craddock et al. 1993; Carter et al. 1994). Diagnosis was established, by a dermatologist, on the basis of physical examination and was confirmed by histological examination of a skin biopsy in at least one member of each family. After informed consent was obtained, peripheral blood was collected in EDTA, for DNA isolation, and in acid citrate dextrose, for the establishment of Epstein-Barr virus–transformed lymphocytes, by standard methods.

Polymorphic microsatellite markers.—Twenty-three polymorphic DNA markers between D12S105 and D12S129 were used in this study (fig. 1*e*). The order of these markers was determined on the basis of both physical analysis of the region and genetic analysis of the families studied here. Nine of these markers (D12S2398, D12S2392, D12S2257, D12S2393, D12S2395, D12S2263, D12S2273, D12S2396, and D12S2397) are new polymorphic repeats isolated from PACs and BACs to more precisely localize the DD gene.

Isolation of new polymorphic markers from PAC and BAC clones.—A microsatellite-rescue technique adapted from Munroe et al. (1994) was used to isolate $(CA)_n$ repeats from PAC and BAC clones. Five hundred nanograms of PAC or BAC DNA was digested with blunt-cutting restriction enzymes (*Alu*I, *Hae*III, and *Rsa*I) and was ligated to a blunt-ended bubble oligonucleotide. This vectorette library was used for PCR amplification using a $(CA)_{11}$ primer and the vectorette primer. The PCR products were sequenced, and a first specific primer was designed downstream of the repeat sequence. This primer was used for PCR amplification of the entire CA repeat. The PCR products were sequenced, and a second specific primer upstream of the repeat was designed to PCR amplify the repeat from genomic DNA. Other repeats were identified by sequencing of the PAC and BAC ends. Primer sequences for these markers are shown in table 1 and are available from the Genome Database (GDB).

Genotyping of DD pedigrees.—Microsatellite analysis was performed by PCR amplification of 100 ng of genomic DNA in a 40-μl reaction containing 10 pmol each of the forward and reverse primer, 200 μM dNTPs, 1 × reaction buffer (1.5 mM $MgCl_2$, 45 mM Tris pH 8.8, 11 mM $[NH_4]SO_4$ pH 8.8, 6.7 mM β-mercaptoethanol, and 4.5 μM EDTA), and 0.8 U of Ampli*Taq* DNA polymerase (Perkin-Elmer). Amplification was performed after a hot-start procedure, with an initial denaturation at 94°C for 2 min and 30 cycles at 94°C for 30 s, at either 50°C or 55°C for 40 s, and 72°C for 10 s, in an MJ Research PTC-100 thermal cycler. Products were mixed with an equal amount of formamide buffer, were separated on denaturing polyacrylamide gels (National Diagnostics), and were transferred onto a Biodyne B nylon membrane (Pall). The membranes were hybridized with a primer that was $\alpha[^{32}P]$-dCTP end-labeled (3,000 Ci/mmol; Amersham) by means of terminal transferase (Boehringer).

Alternatively, microsatellite markers were amplified by PCR using a $\gamma[^{32}P]$-dATP–labeled primer (>3,000 Ci/mmol; Amersham). PCR products were then subjected to denaturing PAGE (2.5%–6% gels) for 3–4 h, were dried, and were autoradiographed on x-ray film (X-Omat-AR; Kodak).

Physical Mapping

Pulsed-field gel electrophoresis (PFGE).—Long-range restriction mapping was performed by blot hybridization of high-molecular-weight DNA isolated from cell lines derived from DD patients. DNA was digested with *Not*I, *Bss*HII, or *Mlu*I and was fractionated by PFGE in a 1% agarose gel for 22 h at a pulse time of 50–90 s, by means of a CHEF DRII (Bio-Rad) apparatus. After electrophoresis, the DNA was alkali transferred to Amersham Hybond N^+ membranes, and hybridization was conducted with different cDNA clones obtained through the Integrated Molecular Analysis of Genomes and Their Expression (IMAGE; http://www2.ncbi.nlm.nih.gov/dbST/dbest_query.html) consortium and known to map to the critical region. The clones (with derivative EST names

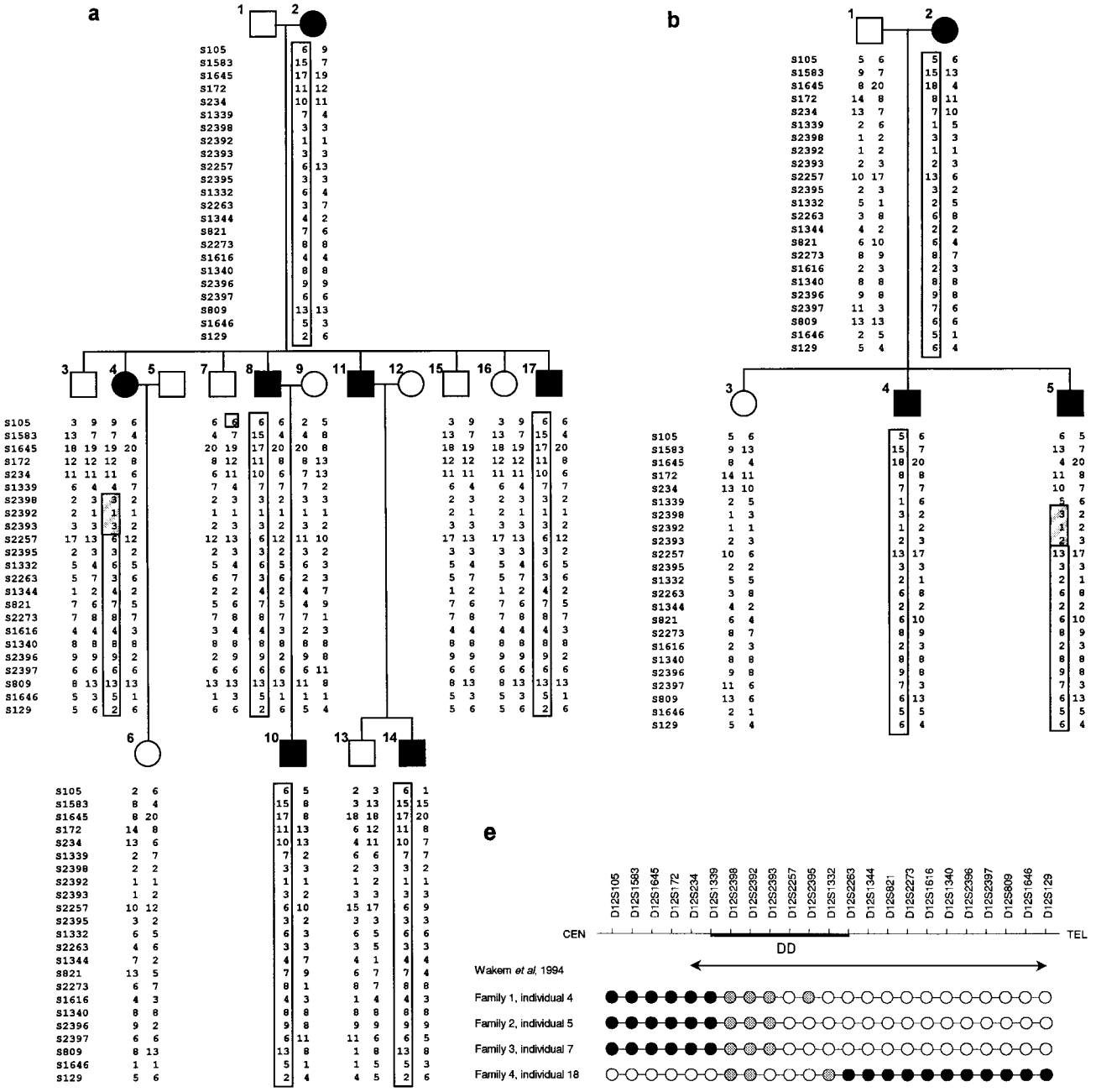

Figure 1 Haplotype analysis of the DD families, showing critical recombinants (*a–d*), and schematic representation of the key recombinant events (*e*). Pedigrees 1 (*a*), 2 (*b*), and 3 (*c*) are French, Irish and Hungarian DD families, respectively, that have not been published elsewhere; pedigree 4 (*d*) has been published (as family "B") by Carter et al. (1994). The boxed alleles are those associated with DD; and the cross-hatched alleles are those adjacent to crossover points, where, because of either homozygosity in the transmitting parent or parental allele sharing, haplotype assignment is not possible. The locus order is from the centromere (*top*) to the telomere (*bottom*). Critical recombinants in individuals 1-4, 2-5, and 3-7 locate the DD locus distal to D12S1339. Recombination events in individual 4-18 place the DD locus proximal to D12S2263. For the deceased individuals (denoted by a diagonal line through the symbol), in pedigrees 3 and 4, the haplotype was inferred. In the schematic representation of the key recombinant events (*e*), the previously published critical region is indicated by the double-headed horizontal arrow, and the recombinants found in the present study are denoted by blackened circles; unblackened circles denote nonrecombinants, gray-shaded circles denote uninformative markers in the critical region, and the new critical DD region is represented by the black horizontal bar spanning the interval from D12S1339 to D12S2263. Note that, in pedigree 3 (*c*), the affected allele for marker D12S1339 is 4 in individuals 9 and 10 but is 7 in individuals 1–3, which is likely to be due to a new deletion occurring within the CA repeat, either in individual 1 or in the mother of individuals 1 and 8; and, in pedigree 4 (*d*), the affected allele for marker D12S1344 is 3 in individual 7 but is 5 in all other affected individuals from this family, which is expected to be due to lengthening of this microsatellite in individual 7.

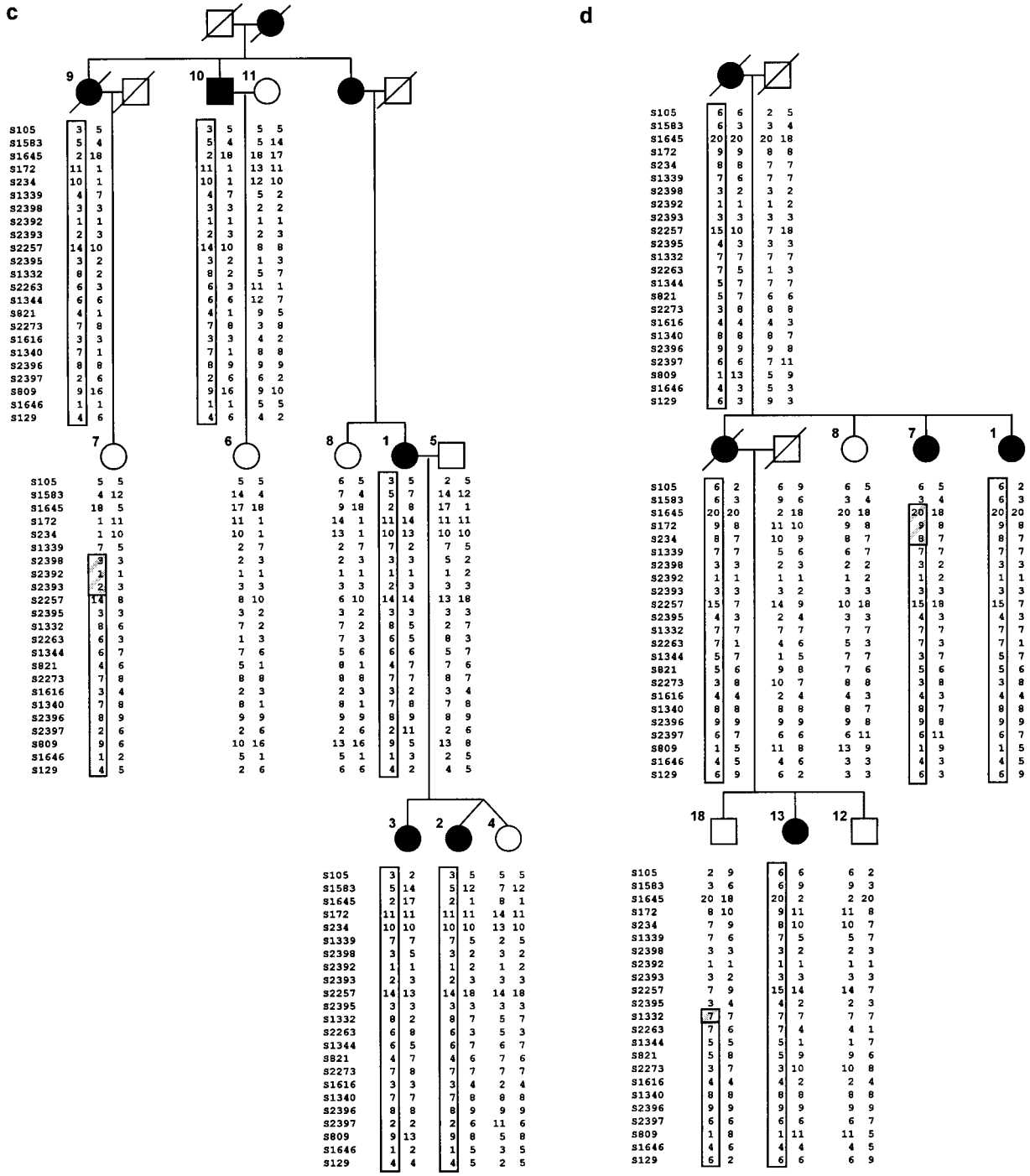

Figure 1 (*continued*)

in parentheses) were 122093 (WI-14197), 119977 (SGC-33766), 214728 (SGC-35037), 32697 (SGC-32083), and 124813 (WI-14804).

Construction of the YAC contig.—YACs were identified from a total human genomic mega-YAC library constructed by CEPH (Dausset et al. 1992) and the Imperial Chemical Industries YAC library (Anand et al. 1989). Library pools were screened, by PCR amplification, for the presence of publicly available sequence-tagged sites (STSs) between D12S105 and D12S129, as well as for the presence of YAC ends and inter-*Alu* PCR products. The CEPH mega-YAC library was also electronically

Table 1

STSs Used for Refined Mapping, and Contig Construction, at DD Locus

Marker	GDB Number	Primer-Sequence Pair (5′→ 3′)		Product Size (bp)	Annealing Temperature (°C)	No. of Alleles Observed in Famulies Studied	Heterozygosity Observed in Families Studied[a]
		Forward	Reverse				
Polymorphic:							
D12S2398 (Y959F8CA)	9120630	ACCAGCAGGCGGAAGAGAAGG	GGGTGACAGGGCGAGACTCCA	287	55	5	.6
D12S2392 (P424M6CCTT)	9120530	ATAGAGACGGGGTTTCGCCA	AGCGGGGGCAGTTATACAAG	250	55	3	NC
D12S2257 (P17E5CA)	5886634	GCTGGTGGGAGTGTCTTTT	GCTGAGATTGTGCTGCTGC	267	55	18	.88
D12S2393 (P150N20TA/CA)	9120533	TCTTTTACACACTACAATCACAG	AGGCACATTTTGAGTTATTTTGG	320	55	3	NC
D12S2395 (P336P3CA)	9120537	TCTCCTTCCCAAGCTGTCC	TTCCCCCAAAACCCTTCTACA	181	50	4	NC
D12S2263 (P462E2CA)	5886644	ACCCCATCTCTACTAAACAC	CAATCTCCTGCCTCACCTT	135	50	12	.81
D12S2273 (P267B10CA)[b]	5886672	TGGGCAACAGAGTGAGAC	GCCCCTTCAACCTTCAAA	175	55	10	.44
D12S2396 (P223G16CA)[b]	9120541	CAGGGATACGCACACACGTA	CATATTGGATGCAGACACTTGCCA	169	55	12	.56
D12S2397 (OASCA)[b]	9120542	GCTTTATGGTATTGACTTGTATC	AATTGAAAGCTAAGTGAGAGAG	216	55	13	.63
Nonpolymorphic:							
D12S2377 (P239L7SP6)	9120484	TTATCACCCCCAAAAGAAATCC	GCTAGTTGCCTTGAGCTAGA	93	58		
D12S2378 (P501B18SP6)	9120487	CAGCCGATACTTTGCCTTTTA	TGACAATACCCTCCCCCGT	160	58		
D12S2379 (B346I4SP6)	9120490	TGAATCACAGACACACGGGG	TTGAGGGAAATGATGAAAATGTA	207	60		
D12S2380 (P7G5SP6)	9120493	AAGGGTAAGCTGAAAGTGAA	AAAGAAGTTGCTCACATCAC	78	55		
D12S2381 (P393M21T7)	9120496	GCTGGGAGGTGCCTTATTG	TTTCTGTCCTCTCCTTCACC	173	50		
D12S2382 (P7G5T7)	9120499	TGCCGACATTGACACACCTG	TCCAGATGCCCAAACCAAAC	82	50		
D12S2399 (P463F12T7)	9120652	GCCCACCTCAGCCTCCCC	AGCAAGGTTTCAGGACACAAG	266	55		
D12S2383 (P82O5CA)[c]	9120502	ATGCCGGGGAACAGCCACT	AACAGAAAATGAAGGACAGGAC	120	60		
D12S2387 (P525K24SP6)	9120514	TGTGCTTCAGTTCCCTTATC	AAGCAAATAACCTGGTACTG	146	55		
D12S2388 (P525K24)	9120517	TGCCACTGCTCTCCATCCT	GTTGAAATTGTAAACTTCTAATCT	420	60		
D12S2400 (525K24T7)	9120655	CTGCTATTTTGTGAGTGCTCC	AGCAAGGTTTCAGGACACAAG	99	55		
D12S2287 (P46F2T7)	5886747	ATAGATAAGGGAACTGAAGCAC	AGGGAGCAGGGAGATGGAG	126	55		
D12S2391 (P256D10CA)[c]	9120525	ATAGCATTTGTGTCTTCTCTTTC	CAGTGGTTAGGAGTGTGGTT	350	50		

[a] NC = not calculated, because these polymorphic markers were tested only with families 1–4.

[b] Marker is telomeric to the critical region (does not appear on the PAC/BAC map [fig. 3]).

[c] Nonpolymorphic repeat.

screened by means of the CEPH-Généthon (http://www.cephb.fr/ceph-genethon-map.html) integrated map.

Construction of the PAC/BAC contig.—In *hybridization-based library screening*, a human genomic PAC library and a BAC library were used to construct this contig. The PAC library was provided by Pieter de Jong and consists of 202,752 clones representing approximately sixfold coverage of the genome (Ioannou et al. 1994). The BAC library was purchased from Research Genetics (Shizuya et al. 1992) and comprises 221,184 clones (eightfold coverage of the genome). Each library was arrayed in duplicate on 12 22 × 22-cm Hybond N^+ nylon membranes.

The PAC and BAC high-density filters were hybridized by use of pooled STSs that were publicly available or that we isolated from ends of either clones or inter-*Alu* sequences. The probes were $\alpha[^{32}P]$-dCTP labeled, and they were tested for the presence of repetitive elements, by hybridization to Southern blots of PAC and BAC clones and human genomic DNA. Probes containing repeats were subsequently competed with human placental DNA prior to library screening. The probes were then hybridized to PAC-library and BAC-library filters in formamide-hybridization buffer (50% formamide, 50 mM $NaHPO_4$ pH 7.2, 4 × SSC, 1% SDS, 8% dextran sulfate, 1 × Denhardt's solution, and 200 μg of degraded herring-sperm DNA/ml). The filters were washed in 0.5% SDS and 0.5 × SSC for 30 min at room temperature and then were rewashed for 30 min at 65°C and were exposed overnight to x-ray film.

Positive clones were picked into 96-well microtiter dishes, gridded onto Biodyne B nylon membranes (Pall), and rescreened by hybridization with individual probes from the probe pool. Positive clones were grown in 10 ml of 2 × YT medium (1.6% bacto-tryptone, 1% bacto-yeast extract, and 0.5% NaCl) containing kanamycin (25 μg/ml), for PACs, or in 10 ml of LB (1% bacto-tryptone, .5% bacto-yeast extract, and 1% NaCl) medium with chloramphenicol (12.5 μg/ml), for BACs. DNA was prepared by means of a modified alkaline-lysis miniprep procedure.

In addition to hybridization, the human PAC and BAC libraries were screened by *PCR-based library screening* that used primers that were specific for STS and that mapped in the region. The human PAC and BAC libraries comprised 321 and 576 plates, respectively, of 96 wells each. PCR conditions were optimized for each set of primers. To confirm the positive clones, three colonies of each positive clone were tested by PCR.

Construction of a cosmid library from YAC 979a5.—A cosmid library was made from YAC 979a5. Whole-YAC DNA was partially digested with *Mbo*I in agarose blocks and was ligated to SuperCos I vector from Stratagene. In vitro packaging was performed with Gigapack II packaging extracts from Stratagene. Cells were plated, and filter lifts were made and hybridized with $\alpha[^{32}P]$-dCTP–labeled total human DNA. Human clones were arrayed on high-density filters that were hybridized with PAC ends.

YAC-, PAC-, and BAC-end recovery.—YAC-end sequences were isolated by a variety of methods. D12S2300 and D12S2301 were recovered by inverse PCR as described by Arveiler and Porteous (1991), by, respectively, *Taq*I and *Pst*I digestion of the YAC DNA. D12S2302 and D12S2303 end sequences were obtained by thermal asymmetric interlaced PCR (Liu and Whittier 1995). YAC-, PAC-, and BAC-end sequences were also isolated by established vectorette-mediated PCR techniques (Riley et al. 1990; Munroe et al. 1994). DNA was digested with *Rsa*I, *Alu*I, and *Hae*III and was blunt-end ligated to double-stranded vectorette, and it also was digested with *Bst*YI and was blunt-end ligated to a *Bam*HI double-stranded vectorette. The vectorette libraries were amplified with both the vectorette primer and a primer for either the right arm or the left arm of pYAC4, for YAC-end recovery, and were amplified with either T7 or SP6 primers for isolation of PAC and BAC ends. Amplified end fragments were $\alpha[^{32}P]$-dCTP radiolabeled by random priming (Megaprime; Amersham). The end fragments that showed DNA fingerprinting were subsequently sequenced, and primers outside the repetitive sequences were designed.

Cosmid-end recovery.—Cosmid DNA was digested with different restriction-endonuclease enzymes that do not cut within the SuperCos I vector; *Kpn*I, *Sac*I, and *Sal*I were used. The digested cosmids were religated and transfected into competent cells. DNA was extracted from transformed cells and was digested with the same enzyme and/or with *Eco*RI, which cuts within the multiple cloning site of SuperCos I. Analysis of the restriction pattern obtained permitted us to identify cosmid ends, which subsequently were gel purified, labeled by random priming, and used as probes for hybridization experiments.

*Inter-*Alu *PCR probes.*—DNA from YACs, PACs, and BACs was amplified with the *Alu* 34 and *Alu* 278 *Alu*-repeat primers, as described by Nelson et al. (1989). Amplification was performed by the Expand Long Template PCR System (Boehringer Mannheim), with PCR conditions recommended by the manufacturer. The PCR products were separated in a 0.8% agarose gel, and the fragments that were not shared by adjacent clones were gel purified, labeled, and used for hybridization.

Analysis of PAC and BAC clones.—Southern blots of *Eco*RI-digested PAC and BAC DNA were used to confirm the overlaps between clones, by hybridization. PFGE separation of *Not*I-digested PAC and BAC clones was used to determine the insert size, as well as the presence of internal *Not*I restriction sites. The digested

samples were run in 1% agarose gels at 6 V/cm for 18 h, at an initial pulse time of 2 s and a final pulse time of 15 s, with a CHEF DRII (Bio-Rad) apparatus.

FISH analysis.—YACs were tested, by FISH analysis, for chimerism. One microgram of DNA was biotinylated by nick translation with the Bionick Labelling System (Life Technology) and was processed by standard techniques. To confirm the chromosome 12 localization, sequences from chromosome 12 (Oncor) were hybridized simultaneously or sequentially. A minimum of 10 metaphases were scored for each sample.

Results

Search for Gross Rearrangements

Our detailed cytogenetic analyses in samples from 43 unrelated DD patients failed to reveal any disease-associated chromosomal abnormalities. In addition, extensive long-range restriction mapping involving hybridization of five different probes from the DD critical region to PFGE Southern blots of DNA samples from 56 unrelated patient samples failed to reveal any evidence of large-scale rearrangements (data not shown). As a result, we sought to extend our genetic analysis, in an effort to reduce the critical region and to create detailed physical and transcript maps to expedite identification of the DD gene.

Genotyping Analysis

We have genotyped members of 41 DD families comprising 397 individuals, 216 of whom are affected. A total of 23 polymorphic DNA markers mapping between D12S105 (AFM262xb9) and D12S129 were used in this study. These markers include nine new polymorphic microsatellites that we isolated, as the contig was being assembled, from YAC or PAC clones mapping in the region. The primer sequences, size of the PCR product, number of alleles, and percent heterozygosity of the new polymorphic markers are indicated in table 1. Critical meiotic recombination events were found in four unrelated families, which allowed us to refine the genetic interval of the DD gene (fig. 1). One affected individual in each of three families (individuals 1-4, 2-5, and 3-7, shown in fig. 1*a–c*, respectively) showed recombination events with the centromeric markers D12S105, D12S1583, D12S1645, D12S172, D12S234, and D12S1339 (AFM240we1). This places the DD locus distal to D12S1339. One family member (4-18; fig. 1*d*) showed evidence of recombination with the telomeric markers D12S129, D12S1646 (AFMb023yd5), D12S809, D12S2397, D12S2396, D12S1340, D12S1616 (AFM219zg5), D12S2273, D12S821, D12S1344 (AFMa154tc5), and D12S2263. This recombinant event occurred in a 60-year-old man who has been closely examined by a dermatologist. The unaffected status of this individual is certain, since penetrance of the disease is considered to be complete at his age. The evidence from this individual localizes the DD locus proximal to D12S2263. According to the Généthon (http://www.genethon.fr) map of chromosome 12 (Dib et al. 1996), these results refine the location of the DD gene to a critical interval of<1 cM, which is flanked by the centromeric marker D12S1339 (AFM240we1) and the telomeric marker D12S2263 (fig. 1*e*). Since no common haplotype was observed in affected individuals from the various families studied (data not shown), linkage disequilibrium was not evident in these families.

YAC-Contig Construction

To develop a physical map of the region containing the DD locus, 25 markers publicly available and located between D12S105 and D12S129 were used to screen the CEPH YAC library. Twenty-nine YACs were first identified either by an electronic search of the CEPH-Généthon database or by PCR screening of the CEPH mega-YAC library (fig. 2). These YACs were subsequently tested for the presence of 10 additional STSs more recently mapped in the region. A partial contig containing a gap between *PPP1CC* and D12S1333/1344 could then be constructed. In an attempt to connect the two groups of YACs, new clones were identified from the CEPH and the Imperial Chemical Industries YAC libraries, by use of the existing markers and new STSs derived from YAC clones. Eight new STSs (D12S2289, D12S2300, D12S2301, D12S2302, D12S2303, D12S2307, D12S2308, and D12S2309) were generated from the ends of YACs, and four STSs (D12S2298, D12S2304, D12S2305, and D12S2398) were isolated from inter-*Alu* sequences (fig. 2); the use of these new STSs led to the identification of 2 and 12 YAC clones from the CEPH and the ICI YAC libraries, respectively, which confirmed links between original clones and improved coverage of the region (fig. 2). The YAC contig was not complete, however, because of a gap, in clone representation, in the interval between D12S2301 and D12S2308. Two YACs (748e12 and 959f8) crossed this gap but showed deletions for markers D12S2301 and D12S2308; YACs 5HA2 and 884h11 were positive for D12S2308 but negative for D12S2301; and YACs 979a5 and 26IH4 were positive for D12S2301 but negative for D12S2308. FISH analyses revealed that, of the 30 YACs tested in this contig, 11 (699a9, 812h2, 861f12, 887b9, 919a2, 959f8, 979a5, 5HA2, 13HB7, 29CB7, and 31EG1) were confined to chromosome 12, and 19 were chimeric. Eight YACs (748e12, 780c6, 884h11, 919a2, 959f8, 979a5, 22GE3, and 29CB7) contained deletions, as determined by STS-content mapping (fig. 2).

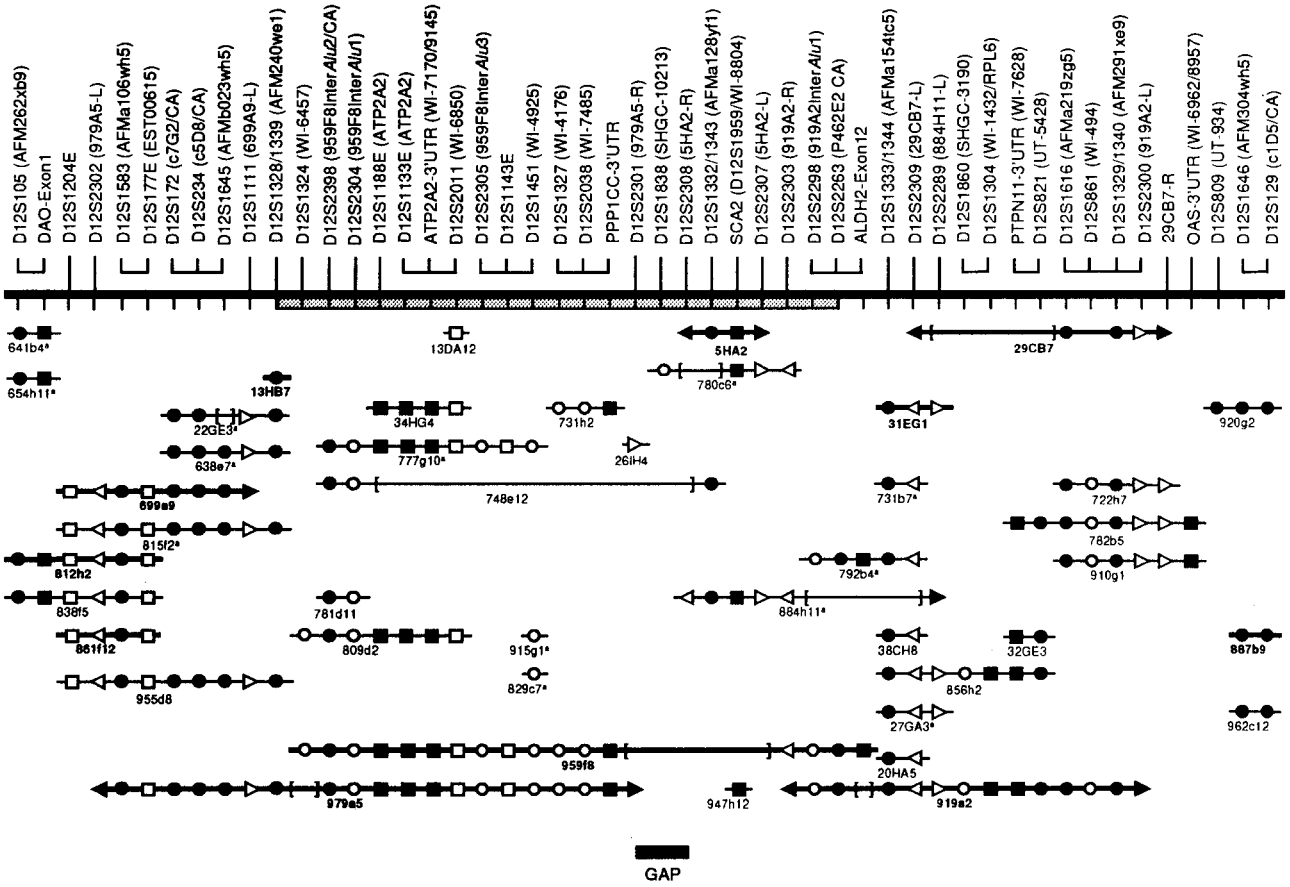

Figure 2 YAC map of the DD region. This map spans the markers from D12S105 to D12S129. Positions of DNA markers are indicated by vertical lines on the top bar, with brackets grouping sets of adjacent markers whose exact order is uncertain. The refined DD region defined in this study is represented by the gray-shaded bar. YACs from the CEPH library are distinguished by a single lowercase letter in their coordinates (e.g., 979a5), whereas YACs from the ICI library have two uppercase letters in their coordinates (e.g., 5HA2). A YAC end is denoted by an arrowhead, which, if it is blackened, denotes that the end originates from this clone. Nonchimeric YACs are indicated by thicker lines with boldface labels, whereas chimeric YACs are denoted by thinner lines. YACs in which chimerism has not been determined are indicated by a superscript "a."Blackened circles denote polymorphic markers; unblackened circles denote nonpolymorphic STSs; blackened squares denote gene-based markers; and unblackened squares denote ESTs. Square brackets denote a deletion within a YAC. The gap between D12S2301 and D12S2308 is indicated by the thickest bar (GAP).

PAC/BAC Contig Construction

To overcome the deficiency in the YAC-clone contig and to provide a more efficient template for gene identification and DNA sequencing, a bacterial-clone contig was constructed. PAC and BAC libraries were screened with 21 known STSs and 13 new STSs, derived from YACs that mapped in the region (fig. 2). This led to the generation of 10 STS-anchored islands of PAC and BAC clones, from which walking strategies were developed. To link these islands, a total of 34 new STSs were generated from these clones. These new STSs comprised 25 vectorette-rescued end clones, 10 of which were sequenced, enabling primers to be designed for PCR amplification (table 1). Ten other PAC ends and five BAC ends were used directly as probes, either for establishment of overlaps or to isolate new clones. Other new STSs included six polymorphic repeats, two nonpolymorphic repeats (D12S2383 and D12S2391), and one anonymous STS (D12S2387) (table 1). Each probe was hybridized to gridded PAC and BAC sublibrary filters and to Southern blots of *Eco*RI digests of clones derived from the corresponding islands. Some probes, such as P424M6T7, P46F2T7, P46F2SP6 , P508G24SP6, and P256D10T7, directly connected islands. Other probes hybridized only to clones on the same side of a gap and therefore were used to rescreen the PAC and BAC libraries. With this clone walking strategy, 7 of the 10 islands were linked. In particular, complete coverage of the region spanning D12S2301 and D12S2308, which was not represented in YAC clones, was obtained by the

identification of four groups of overlapping PAC and BAC clones and the use of 14 STSs (fig. 3). However, a region between D12S1339 (AFM240we1) and D12S2399 proved to be particularly difficult to cover. Screening of the PAC and BAC libraries by end clones from PACs flanking this gap failed to identify positive clones. In contrast, screening of a cosmid library made from YAC 979a5, which covers this region, gave several positive clones (C1F13 and C1F17). Screening of the PAC and BAC libraries with three end probes from these cosmids permitted us to identify P7G5, whose ends were successfully used to walk toward P463F12.

Mapping of Genes and ESTs

The two remaining gaps—that between D12S1332 and D12S2307 and that between D12S2309 and D12S2289—were linked by mapping known genes and ESTs in the region. Seven genes (*ATP2A2, PPP1CC, SCA2, ALDH2, RPL6, PTPN11,* and *OAS*) and 62 ESTs mapped between D12S105 and D12S129, according to the human transcript map. Primer sequences for the seven genes were obtained from GDB and were used to generate gene-specific PCR products. These products were labeled and used as hybridization probes across the contig. The cDNA inserts from the 62 EST clones were isolated and also probed to our contig. Four genes (*ATP2A2, PPP1CC, SCA2,* and *ALDH2*) and 17 ESTs mapped between D12S1583 and D12S1860, but only three of these genes (*ATP2A2, PPP1CC,* and *SCA2*) and 10 ESTs mapped in the critical region between D12S1339 and D12S2263 (fig. 3). In particular, *SCA2* and ESTs R43605 and R65814 linked D12S1332 to D12S2307 within the critical region, whereas ESTs W91999, R13589, H05663, R37746, H98770, and AA082344 established an overlap between D12S2309 and D12S2289, which are located telomeric to the critical interval (fig. 3).

Validation of the Contig and Estimation of Its Size

The combination of the mapping of end clones, inter-*Alu* probes, anonymous STSs, polymorphic markers, genes, and ESTs resulted in the construction of a complete contig extending from D12S1583 to D12S1860. This contig consists of 35 YACs, 69 PACs, 16 BACs, and 2 cosmids spanning the region containing the DD gene. To validate this contig, which was constructed by STS-content mapping, we performed *Eco*RI restriction-fragment fingerprinting of 16 PAC and 2 BAC clones forming the minimal tiling path of the critical region between D12S1339 and D12S2263. This provided further evidence for overlaps between these clones and confirmed their order. The size of the critical region between D12S1339 and D12S2263 was estimated by adding the insert size of the PAC and BAC clones and subtracting the overlapping fragments obtained after *Eco*RI digestion (table 2). This distance was calculated as ~2.4 Mb.

FISH analysis confirmed chromosomal position, in 12q24.1, for 16 of the 18 PAC clones tested (P239L7, P17K1, B346I4, P501B18, P463F12, P82O5, P525K24, P365O9, P17E5, P74B13, P46F2, P336P3, P440L2, P287C7, B42B1, and P462E2 [data not shown]); the other 2 clones (P316E13 and P325G22), which initially had been placed in the contig, by both hybridization and PCR analysis, mapped in 12q22 and therefore were not included in our contig.

Discussion

We have refined the genetic interval containing the DD locus on chromosomal region 12q23-24.1 and have constructed a high-resolution PAC/BAC contig of this region. Analysis of key recombinants in DD families reduces the candidate region for DD, from 2 cM to a region of<1 cM, between D12S1339 and D12S2263. It should be noted that the centromeric boundary was established by the identification of recombinants in three affected individuals from different families, whereas the telomeric boundary is based on recombination events in one unaffected individual. However, after careful examination by a dermatologist, this individual was diagnosed as unaffected, at age 60 years—an age at which penetrance of the disease is considered to be complete. Therefore, we believe that both boundaries are real. There was no evidence for a founder effect, on the basis of the haplotype analysis, which showed no allelic association to DD in the families studied. To further narrow this interval, we isolated six new polymorphic repeats from YAC, PAC, and BAC clones within the critical region. The families that we studied were uninformative, rather than nonrecombinant, for the new repeats closest to the flanking markers (fig. 1*e*). Therefore, the discovery of additional informative polymorphic markers in this region may allow the critical region to be narrowed further. Alternatively, the new polymorphic markers described here may prove useful in further refining of the DD locus in other recombinant families.

Our contig now provides complete coverage of the DD region, with PACs, BACs, and cosmid clones between D12S1339 and D12S2263. The use of PAC and BAC clones enabled us to close, in the YAC contig, a gap of ~515 kb, located between D12S2301 and D12S2308. The map that we present also covers a region, between markers D12S1339 (AFM240we1) and D12S2399, that was not represented in two physical maps recently published (Nechiporuk et al. 1997; Renault et al. 1997). On the basis of our results, the size of this region is ~290 kb, which is consistent with the estimate made by Nechiporuk et al. (1997). This region

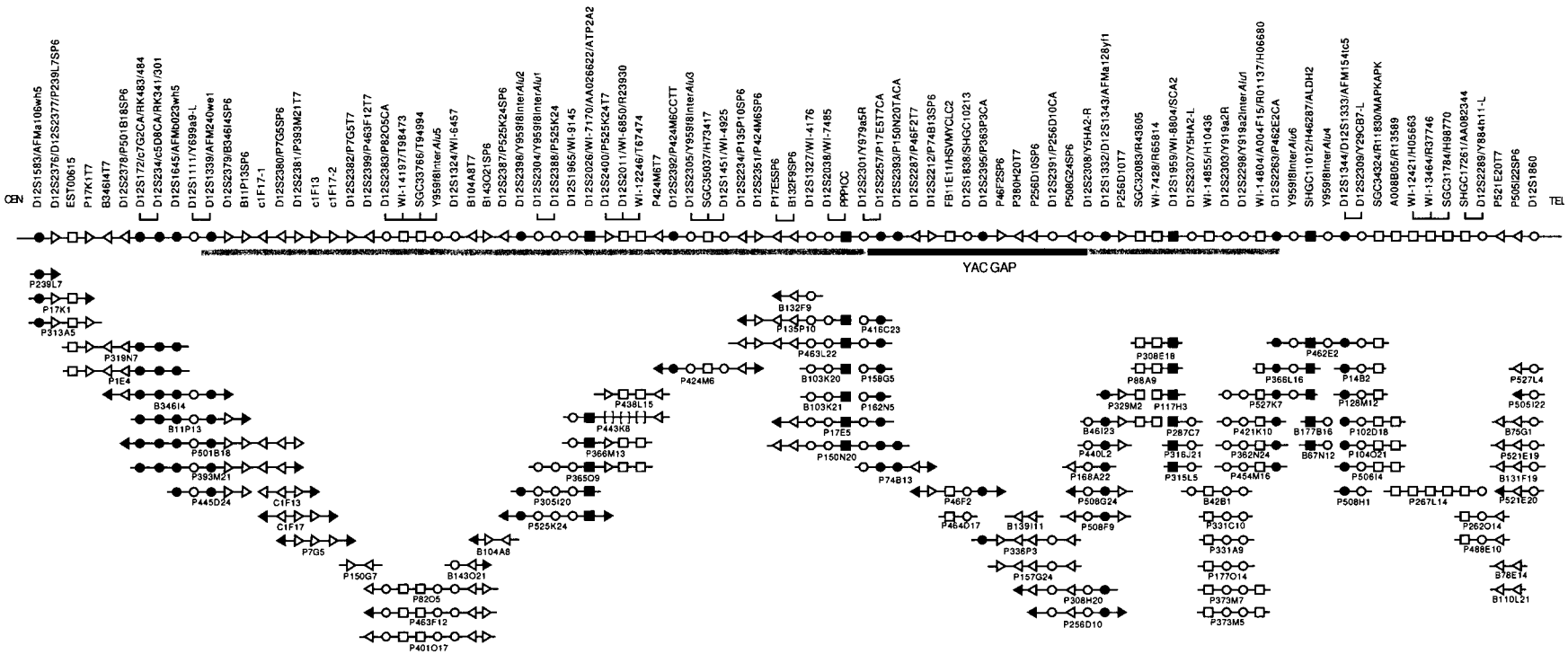

Figure 3 PAC/BAC contig covering the DD gene region. The 88 STSs are listed across the top, with brackets grouping adjacent markers whose exact order could not be determined; these STSs consist of 13 polymorphic repeats, 7 YAC ends, 23 PAC ends, 5 BAC ends, 3 cosmid-end clones, 7 inter-*Alu* repetitive elements, 17 ESTs, 4 genes, and 9 anonymous STSs. "SP6" and "T7" denote the ends of the PAC clones and the BAC clones, respectively. P = PAC; B = BAC; L = left arm of YAC clone; and R = right arm of YAC clone. Arrowheads denote PAC and BAC ends and are blackened to specify the clone from which they were isolated. The gap present in the YAC map is represented by the thicker horizontal bar; and the minimum region containing the DD gene is spanned by D12S1339 and D12S2263 and is represented by the grey-shaded horizontal bar. Blackened circles denote polymorphic repeats; unblackened circles denote nonpolymorphic STSs; blackened squares denote known genes; and unblackened squares denote ESTs. Square brackets denote a deletion within the clone.

Table 2

Estimation of Size of Minimal Tiling Path

Clone Designation	Size(s) of (kb)		
	Clone[a]	Individual Overlapping Fragment(s)	All Overlapping Fragments[b]
P393M12/P7G5	140	5.2, 3.4	8.6
P7G5/P150G7	190	13, 10, 6.5, 5.6, 4.4, 2	41.5
P150G7/P82O5	160	5.2, 5, 2.4	12.6
P82O5/B104A8	130	11, 6.6, 5.6, 3.8	27
B104A8/P525K24	75	7, 4.4, 4.2, 3.2	18.8
P525K24/P443K8	135	3.2, 2.2	5.4
P443K8/P424M6	115	6, 1.8, 1.6	9.4
P424M6/P463L22	115	7.4	7.4
P463L22/P74B13	200	12, 5.2	17.2
P74B13/P46F2	100	11	11
P46F2/P336P3	145	9.5	9.5
P336P3/P508G24	150	7.2, 6, 5.8, 1.8	20.8
P508G24/P329M2	170	11, 10	21
P329M2/P88A9	75	7	7
P88A9/P316J21	145	5.2	5.2
P316J21/B42B1	185	9	9
B42B1/P527K7	250	13, 12	25
P527K7	170		
Total	2,650		256.4

Note.—The distance between D12S1339 and D12S2263 was estimated by subtracting the overlapping fragments from the total insert size of the PAC and BAC clones forming the minimal tiling path and was calculated to be 2,393 kb.

[a] The size given refers to the first clone designation in the column to the left and was estimated on the basis of PFGE of *Not*I digests.

[b] Overlaps between clones were calculated by summation of the size of the *Eco*RI restriction fragments common to those clones.

was difficult to cover, probably because of the repetitive nature of its flanking sequences. Indeed, PAC ends flanking this gap were rich in *Alu* and other repetitive sequences, and their use in screening procedures failed to identify positive clones from the human PAC and BAC libraries. In contrast, screening the more specific cosmid library made from YAC 979a5 led to the identification of cosmid clones, outside the repetitive regions, from which probes could be designed. The observation that this gap could not be filled by screening a 20-genome-equivalent human PAC library (Nechiporuk et al. 1997) suggests that increasing the specificity of the library, as has been done with this YAC-derived cosmid library, improved screening efficiency. The contig that we present also covers another gap, between D12S2385 (463F12SP6) and D12S2398, which was present in the map reported by Renault et al. (1997).

The present map extends from D12S1583 to D12S1860 and consists of 35 YAC, 69 PAC, 16 BAC, and 2 cosmid clones. This region comprises 88 markers, including 50 new STS markers, 32 of which have been sequenced. The critical region extends from D12S1339 to D12S2263, contains 64 STSs, and encompasses ~2.4 Mb, with an average marker resolution of 37.5 kb. Construction of the YAC contig was based on PCR amplification of YAC libraries by means of STS primers. For the assembly of the PAC/BAC contig, we used an approach based on a combination of hybridization and PCR amplification. The hybridization of PAC and BAC high-density filters with clone insert ends isolated by vectorette PCR circumvented the need for sequencing the ends for the development of STSs. The links between PAC and BAC clones were subsequently confirmed by hybridizing Southern blots of *Eco*RI digests of PAC and BAC clones. For STSs containing repetitive sequences, such as *Alu* or long interspersed nuclear elements, PCR products were sequenced, and primers were designed outside the repetitive elements for PCR amplification. These primers were used to confirm existing overlaps and for walking strategies by means of PCR screening and hybridization procedures. The contig was verified by both *Eco*RI restriction-fragment fingerprinting of the minimal tiling path and FISH analysis. There was a good agreement between all four methods, except in the case of PAC clones P316E13 and P325G22 (data not shown); these two clones shared several STSs and had been placed in the contig by both hybridization and PCR. However, they were found by FISH analysis to lie cen-

Table 3

Genes and ESTs Mapping to the DD Region

A. Genes

Gene	GenBank Number	EST NCBI Number	EST IMAGE Number[a]	EST GenBank Number
ATP2A2	119717	WI-7170	366533	AA026622
PPP1CC	135661	SHGC11024	29839	R15137
SCA2	128034	WI-8804	73509	T55469
ALDH2[b]	119668	SHGC11012	178359	H46287
RPL6[b]	139231	WI-1432	…	D58232
PTPN11[b]	677601	WI-7628	650696	D13540
OAS[b]	119465	WI-6962	200521	H48431

B. ESTs

NCBI Number	IMAGE Number[a]	GenBank Number		Tentative Human Consensus-Sequence *P* Value[c]	Length of Tentative Human Consensus Sequence (bp)	Putative Identity BLASTX *P* Value[d]
WI-14197	122093	T98473	…	…	…	…
SGC-33766	28410	R40634	…	…	…	…
WI-6850	131110	R23930	…	…	…	*Homo sapiens* ferritin heavy chain
WI-12246	…	T67474	…	…	…	…
SGC-35037	613048	AA181634	…	…	…	…
FB11E11	…	T02836	…	…	…	*Homo sapiens* ventricular light chain 2 (7.8e-56)
SGC-32083	32697	R43605	2.7e-147	117865	428	…
WI-17428	429293	R65814	1.7e-126	181329	571	Spliceosome-associated protein 49 (9.5e-7)
WI-14855	…	H10436	…	…	…	…
WI-14804	124813	R01137	4.7e-158	147986	493	…
SGC-34324[b]	26026	R11830	…	…	…	Mitogen-activated protein kinase–activated protein kinase 2
A008B05[b]	26630	R13589	5.2e-177	104193	454	…
WI-12421[b]	43982	R41417	1.5e-96	110731	493	…
WI-13464[b]	26914	R37746	1.2e-87	190299	1346	…
SGC-31784[b]	261621	D25662	6.3e-169	178998	1217	Endoplasmic reticulum protein 31
SGHC-17261[b]	366097	AA082344	4.9e-64	179699	1776	…

NOTE.—Genes and ESTs are listed according to position in the contig, from the centromere to the telomere. The NCBI (National Center for Biotechnology Information) numbers and the corresponding GenBank numbers were obtained from the NCBI's UniGene and EST databases; the URLs are http://www.ncbi.nlm.nih.gov/Unigene/index.html and http://www.ncbi.nlm.nih.gov/dbEST/index.html. In many cases there were several GenBank numbers corresponding to the same NCBI number and putative identity, but only one of them is given here.

[a] Obtained from IMAGE; GenBank or NCBI numbers were used to obtain the relevant IMAGE numbers.

[b] Maps outside the critical region.

[c] Obtained by sequence search of The Institute for Genomic Research, by means of EST sequences from NCBI. Reports were generated to give sequence length. Some clones were part of more than one Tentative Human Consensus sequence, but only that with the highest *P* value is given here.

[d] Obtained from BLAST (Basic Local Alignment Search Tool) searches of the NCBI sequence of THC.

tromeric to the DD region, on chromosome 12q22, suggesting that these PACs contain a duplicated DNA sequence localized outside the DD region.

Of the 43 YACs included in the contig (fig. 2), 8 showed deletions, and only 11 of 30 YACs studied by FISH analysis were shown to map exclusively to 12q24. In contrast, only 1 PAC clone (P443K8), among 69, and 0 of the 16 BAC clones showed deletion, on the basis of their STS content. None of the 18 PAC clones tested by FISH were found to be chimeric. These results are in

agreement with the notion that PAC and BAC clones are generally stable and nonchimeric, thus providing powerful tools for the construction of physical maps.

The localization of DD between D12S1339 and D12S2263 excludes several known genes, including *ALDH2, RPL6, PTPN11,* and *OAS,* which map telomeric to the critical region (figs. 2 and 3 and table 3). It also excludes a new member of the *MAPK2* family, corresponding to EST R11830, whose full-length cDNA was cloned and investigated for evidence of mutations in DD patients, prior to linkage analysis (authors' unpublished results). The DD gene may encode a cell-adhesion molecule possibly involved in the integrity of the desmosomal-keratin complex, but, at present, there is no plausible candidate gene or EST known to map to the refined critical region. The plakophilin 2 gene, which codes for a recently described desmosomal plaque protein (Mertens et al. 1996), does not map to this contig (data not shown). The *ATP2A2* and *PPP1CC* genes map in the region but are ubiquitously expressed genes coding for enzymes unlikely to be involved in the disease, whereas the *SCA2* gene is not a likely candidate, since CAG expansion in this gene is known to cause spinocerebellar ataxia (Pulst et al. 1996), which shares no common phenotype with DD (table 3). Among the 17 ESTs that we have mapped between D12S1339 and D12S1860, only 10 localize within the critical region (fig. 3 and table 3), and 0 show sequence similarity with known structural genes involved in cell-to-cell adhesion. However, prior to full-length cDNA cloning and sequencing, the possibility that one of them is a candidate gene cannot be excluded. Therefore, these ESTs are currently being investigated for expression in keratinocytes. It is also likely that the large-scale sequencing of this region will identify additional ESTs and predicted exons.

The chromosomal 12q24.1 region is expected to be a gene-rich region, on the basis of its light banding after Giemsa staining. The 2.4-Mb region that we have delineated may thus contain as many as 80 genes, and only 3 known genes and 10 ESTs have been mapped in the minimal region. Therefore, the isolation of new expressed sequences by exon trapping, cDNA selection, and direct hybridization of PAC and BAC inserts to keratinocyte cDNA libraries is currently being performed in our laboratories. In addition, the PAC/BAC contig that we have constructed is a valuable source for gene identification based on large-scale genomic sequencing.

The identification of the DD gene will provide insights into the mechanisms of cell-to-cell adhesion and of normal differentiation of the epidermis. Its identification will possibly help in the understanding of the pathophysiology of some of the neuropsychiatric disorders associated with the disease. The systematic search for genes in the DD region may also lead to the identification of other disease-causing genes that map to this region; these include the genes underlying the Noonan syndrome (Jamieson et al. 1994) and scapuloperoneal spinal muscular atrophy (Isozumi et al. 1996), which have been mapped between D12S84 and D12S366 in a region encompassing the DD locus. Therefore, the refined genetic and physical map of chromosome 12q24.1 presented here provides important tools for the identification of the DD gene and, possibly, other disease genes.

Acknowledgments

We are grateful to Jo Pang, Rebecca Twells, and Sue Chamberlain for providing markers D12S2307, D12S2308, and D12S2309 and for providing data from their FISH analyses using YACs from the DD/*SCA2* critical region. We would like to thank Beatrice Renault, Raju Kucherlapati, and their colleagues for providing unpublished data from their chromosome 12 physical mapping project. We acknowledge Dr. Dominique Bonneau for organizing the collection of DNA samples from family 1. We are thankful to Robin Butler, Eileen Fraser, and Jayne Wu for their help in cosmid-library construction, isolation of polymorphic markers, and FISH analysis, respectively. We are indebted to the U.K. Human Gene Mapping Resource Centre, to the CEPH, and to Pieter de Jong for providing useful clone resources for this project. S.M. is supported by a Wellcome Trust prize studentship; A.S. is supported by the Royal Thai Government and the faculty of Medicine, Ramathibodi Hospital, Mahidol University, Bangkok; A.P.M. and M.L. are Wellcome Principal Research Fellows; T.S., C.S.M., and J.L.R. gratefully acknowledge Wellcome Trust Project grant support for S.A.C. and S.B.; R.C., L.H., and E.L. are supported by the Wellcome Trust; V.L.R.-P. is supported by an EC TMR fellowship; and A.H. held a Wellcome Trust and an EC research fellowship.

References

Anand R, Villasante A, Tyler-Smith C (1989) Construction of yeast artificial chromosome libraries with large inserts using fractionation by pulsed field gel electrophoresis. Nucleic Acids Res 17:3425–3433

Arveiler B, Porteous DJ (1991) Amplification of end fragments of YAC recombinants by inverse-polymerase chain reaction. Technique 3(1): 24–28

Bashir R, Munro CS, Mason S, Stephenson A, Rees JL, Strachan T (1993) Localisation of a gene for Darier's disease. Hum Mol Genet 2:1937–1939

Burge S, Garrod DR (1991) An immunohistological study of desmosomes in Darier's disease and Hailey-Hailey disease. Br J Dermatol 124:242–251

Burge S, Wilkinson DJ (1992) Darier-White disease: a review of the clinical features in 163 patients. J Am Acad Dermatol 27:40–50

Carter SA, Bryce SD, Munro CS, Healy E, Bashir R, Weissenbach J, Leblanc-Straceski J, et al (1994) Linkage analyses in British pedigrees suggest a single locus for Darier disease and narrow the location to the interval between D12S105 and D12S129. Genomics 24:378–382

Craddock N, Dawson E, Burge S, Parfitt L, Mant B, Roberts

Q, Daniels J, et al (1993) The gene for Darier's disease maps to chromosome 12q23-q24.1. Hum Mol Genet 2: 1941–1943

Craddock N, Owen M, Burge S, Kurian B, Thomas P, McGuffin P (1994) Familial cosegregation of major affective disorder and Darier's disease (keratosis follicularis). Br J Psychiatry 164:355–358

Dausset J, Ougen P, Abderrahim H, Billault A, Sambucy JL, Cohen D, Le Paslier D (1992) The CEPH YAC library. Behring Inst Mitt 91:13–20

Dib C, Fauré S, Fizames C, Samson D, Drouot N, Vignal A, Milasseau P, et al (1996) A comprehensive genetic map of the human genome based on 5,264 microsatellites. Nature 380:152–154

Goldsmith LA, Wakem P, Polakowska R, Haake A, Ewing N, Sarret Y, Trattner A, et al (1993) Exclusion of candidate genes in Darier's disease using positional cloning. J Invest Dermatol 101:458

Ikeda S, Wakem P, Haake A, Ewing N, Polakowska R, Sarret Y, Trattner A, et al (1994) Localization of the gene for Darier disease to a 5-cM interval on chromosome 12q. J Invest Dermatol 103:478–481

Ioannou PA, Amemiya CT, Garnes J, Kroisel PM, Shizuya H, Chen C, Batzer MA, et al (1994) A new bacteriophage P1-derived vector for the propagation of large human DNA fragments. Nat Genet 6:84–89

Isozumi K, DeLong R, Kaplan J, Deng H-X, Iqbal Z, Hung W-Y, Wilhelmsen KC, et al (1996) Linkage of scapuloperoneal spinal muscular atrophy to chromosome 12q24.1-q24.31. Hum Mol Genet 5:1377–1382

Jamieson CR, van der Burgt I, Brady AF, van Reen M, Elsawi MM, Hol F, Jeffery S, et al (1994) Mapping a gene for Noonan syndrome to the long arm of chromosome 12. Nat Genet 8:357–360

Liu Y-G, Whittier RF (1995) Thermal asymmetric interlaced PCR: automatable amplification and sequencing of insert end fragments from P1 and YAC clones for chromosome walking. Genomics 25:674–681

Mertens C, Kuhn C, Franke WW (1996) Plakophilins 2a and 2b: constitutive proteins of dual location in the karyoplasm and the desmosomal plaque. J Cell Biol 135:1009–1025

Munro CS (1992) The phenotype of Darier's disease: penetrance and expressivity in adults and children. Br J Dermatol 127:126–130

Munroe DJ, Haas M, Bric E, Whitton T, Aburatani H, Hunter K, Ward D, et al (1994) IRE-Bubble PCR: a rapid method for efficient and representative amplification of human genomic DNA sequences from complex sources. Genomics 19: 506–514

Nechiporuk T, Nechiporuk A, Sahba S, Figueroa K, Shibata H, Chen X-N, Korenberg JR, et al (1997) A high-resolution PAC and BAC map of the SCA2 region. Genomics 44: 321–329

Nelson DL, Ledbetter SA, Corbo L, Victoria MF, Ramirez-Solis R, Webster TD, Ledbetter DH, et al (1989) *Alu* polymerase chain reaction: a method for rapid isolation of human-specific sequences from complex DNA sources. Proc Natl Acad Sci USA 86:6686–6690

Parfitt E, Burge S, Craddock N, Roberts E, McLean WHI, Weissenbach J, McGuffin P, et al (1994) The gene for Darier's disease maps between D12S78 and D12S79. Hum Mol Genet 3:35–38

Pulst S-M, Nechiporuk A, Nechiporuk T, Gispert S, Chen X-N, Lopes-Cendes I, Pearlman S, et al (1996) Moderate expansion of a normally biallelic trinucleotide repeat in spinocerebellar ataxia type 2. Nat Genet 14:269–276

Renault B, Hovnanian A, Bryce S, Chang J-J, Lau S, Sakuntabhai A, Monk S, et al (1997) A sequence ready physical map of a region of 12q24.1. Genomics 45:271–278

Riley J, Butler R, Ogilvie D, Finniear R, Jenner D, Powell S, Anand R, et al (1990) A novel, rapid method for the isolation of terminal sequences from yeast artificial chromosome (YAC) clones. Nucleic Acids Res 18:2887–2890

Shizuya H, Birren B, Kim U-J, Mancino V, Slepak T, Tachiiri Y, Simon M (1992) Cloning and stable maintenance of 300-kilobase-pair fragments of human DNA in *Escherichia coli* using an F-factor-based vector. Proc Natl Acad Sci USA 89: 8794–8797

Wakem P, Ikeda S, Haake A, Polakowska R, Ewing N, Sarret Y, Duvic M, et al (1996) Localization of the Darier disease gene to a 2-cM portion of 12q23-24.1. J Invest Dermatol 106:365–367